European Journal of Environmental and Civil Engineering

ISSN: (Print) (Online) Journal homepage: https://www.tandfonline.com/loi/tece20

Flexural behavior of reinforced concrete beam using CFRP hybrid system

Ala' Taleb Obaidat

To cite this article: Ala' Taleb Obaidat (2021): Flexural behavior of reinforced concrete beam using CFRP hybrid system, European Journal of Environmental and Civil Engineering, DOI: 10.1080/19648189.2021.1934552

To link to this article: https://doi.org/10.1080/19648189.2021.1934552

Published online: 21 Jun 2021.

EUROPEAN JOURNAL OF ENVIRONMENTAL AND CIVIL ENGINEERING
https://doi.org/10.1080/19648189.2021.1934552

Flexural behavior of reinforced concrete beam using CFRP hybrid system

Ala' Taleb Obaidat

Civil Engineering Department, Philadelphia University, Amman, Jordan

ABSTRACT

This paper presents experimental and numerical study to investigate the flexural behaviour of strengthened RC beams using three CFRP techniques. Considered main variables were CFRP technique, amount of CFRP NSM and rope and cost/increase in strength effectiveness. Results indicate that using CFRP rope and sheet increased significantly maximum load and maximum strain of RC beams. Average increase in strength and maximum strain were 76.3% to 143.5% and 206% to 246% as the control RC beam. Moreover, RC beams strengthened with CFRP rope exhibited strength approximately similar to ones strengthened with CFRP strip. The cost/increase in strength ratio of specimens strengthened by CFRP rope is 61% higher than the ratio of specimens strengthened by CFRP NSM strip. Hence, the specimens strengthened by one layer of CFRP rope is the most economic techniques based in cost/increase in strength ratio even though it exhibited maximum load less than the specimens strengthened with two layers of CFRP rope or strip. CFRP rope was 40% lower than CFRP strip when same strengthening effect was achieved. Finally, complementary to experimental work a finite element model FEM was developed to investigate the flexural behaviour of beam. The FEA model showed somehow good agreement with the experimental results.

ARTICLE HISTORY
Received 7 November 2020
Accepted 20 May 2021

KEYWORDS
Carbon Fibre Reinforced Polymers (CFRP); strengthening; reinforced concrete beam; flexure; debonding

1. Introduction

Reinforced concrete (RC) structures constitute the most buildings and bridges around the world. Concrete is one of the most broadly materials utilised in the construction of structure due to its qualities. It has a good quality in compression, however, it is a weak in tension. As a result, a reinforcement steel is placed in tension zone. Moreover, concrete is characterised by a low coefficient of warm extension, economy to form any shape, comprises of popular and available material, and requires less experience for the construction of the structure than steel.

RC beams transmit loads from the floor to the columns which in turn transits the load to foundation. Consequently, Reinforced concrete (RC) beam is one of the most significant element in the structure. However, RC beams deteriorate to several reasons such as excessive loading, reinforcement corrosion, differential settlement and poor design. Hence, the strengthening of RC flexural elements is urgently needed to improve its load carrying capacity and serviceability requirements. Presently, a lot of ongoing research are conducted on strengthening RC structural elements. Literature showed that several techniques have been developed for strengthening/repairing purposes to enhance load capacity and ductility of structural element members. Also, studies showed that one of the most effective material used in strengthening repairing and retrofitting RC elements is carbon Fibre reinforced polymers CFRP. CFRP is

CONTACT Ala' Taleb Obaidat atobaidat@Gmail.com; aobaidat@philadelphia.edu.jo Civil Engineering Department, Philadelphia University, Amman, 19392, Jordan

preferable in strengthening and repairing RC elements due its high tensile strength, low weight, high stiffness and high durability since no corrosion extensively used, and are practically unlimited availability in terms of geometry and size (ACI 440F, 2008; Bakis et al., 2002). However, the CFRP is failed in brittle manner. Recently, studies have addressed that using FRP for strengthening and retrofitting RC elements improved flexural and shear capacity (Ashteyat et al., 2019; Mirmiran & Shahawy, 1997; Obaidat, Ashteyat, & Obaidat, 2020; Obaidat, Ashteyat, Hanandeh, et al., 2020). In addition, studies addressed that FRP materials with epoxy provided an excellent performance in terms of application and durability. In RC beams, FRP sheets are often attached to the tension side for flexural strengthening (Kim & Shin, 2011; Wu et al., 2007; Xiong et al., 2004).

Several techniques of CFRP were developed to strengthened structural elements. These strengthening techniques are sheet fabrics (in situ cured systems) or laminates (pre-cured systems) which is glued externally on the surface of the RC element. However, this technique is mostly failed by premature de-bonding which in turn resulting a reduced flexural capacity (Olivova & Bilcik, 2009). Also, FRP laminate or rod can be inserted into grooves opened on concrete cover which is called (NSM – Near Surface Mounted) in order to overcome the limitation in the externally bonded technique (De Lorenzis & Teng, 2007; Obaidat, Ashteyat, Hanandeh, et al., 2020).

Based on results of studies, it was found that the RC element strengthened by NSM exhibited strength higher than ones strengthened by externally bonded FRP (Bilotta et al., 2015; El-Hacha & Rizkalla, 2004; Sarafraz & Danesh, 2008; Szabó & L. Balázs, 2007). Recently, some studies have been conducted in strengthening and repairing RC elements using new flexible FRP techniques called carbon FRP (CFRP) rope. CFRP rope can be inserted in groove open in concrete cover (Al Rjoub et al., 1988; Ashteyat et al., 2019). Epoxy adhesives are usually used to fix the FRP to concrete surface. The efficiency of these techniques depends significantly on concrete cover resistance for strengthening and repairing. However, concrete cover is the most degraded region in RC element because is exposed to environment conditions.

Many researches used NSM-CFRP strip and rope to investigate flexural and shear behaviour of strengthening RC structural elements (Al Rjoub et al., 1988; Ashteyat et al., 2020; Dias & Barros, 2017; Hassan & Rizkalla, 2003). Based on the experimental results the CFRP NSM and rope strengthening technique significantly amplified the first cracking, yield, and ultimate load carrying capacities of the beams, and remarkably better the specimen's mode failure. Also, using NSM enhanced the flexural and shear capacity of RC structures considering several parameters effect such as number, orientation and type of FRP, groove dimensions, size, and location of NSM and type of adhesive.

Grace et al. (2002) conducted a flexural test on eight strengthened concrete beams to examine the effectiveness and ductility of the developed fabric uniaxial ductile hybrid FRP fabric. The developed hybrid system composed of one type of glass fibre and two types of carbon fibres. It was concluded that beams strengthened with developed hybrid system exhibited a higher ductility and capacity compared to similar beams strengthened with CFRP sheets, fabric, and plates. Xiong et al. (2004) conducted a four point loadings on beams strengthened with a conventional CFRP system and a hybrid CFRP/GFRP system. It was seen that the hybrid CFRP/GFRP system exhibited an increase in the deflection response about 89.7% as the CFRP system. However, the RC strengthened beam using the hybrid system showed a decrease in ductility about 16.2% as control RC beam.

Li et al. (2009) employed a software package to construct a finite element method to investigate numerically the interfacial stress between GFRP sheets and hybrid CFRP. The results showed that the interfacial shear and normal stresses decreases when strengthening RC beams by hybrid FRP at the cut-off point of the FRP sheets that would delay the initiation of debonding. Also, a parametric study was done to investigate the interfacial stresses considering the load effect, modulus of elasticity, epoxy adhesive layer thickness and width of FRP sheet. It was concluded that as the loads and elastic modulus, the interfacial stresses increase. Also, interfacial stresses decrease with the increase of epoxy layer thickness. Finally, it was concluded that there was no significant influence to width of the FRP sheet on the interfacial stresses at the FRP ends.

Hosen et al. (2018) tested under four-point bending a total of seven RC beam specimens including un-strengthened control specimen, and six specimens strengthened by SNSM-CFRP strips to enhance the flexural performance of reinforced concrete (RC) beams. It was concluded that the using CFRP strips for strengthening specimens enhanced the ductility, stiffness, and energy absorption capacity. Moreover, using SNSM-CFRP strips strengthening technique significantly improved the first cracking, yield, and

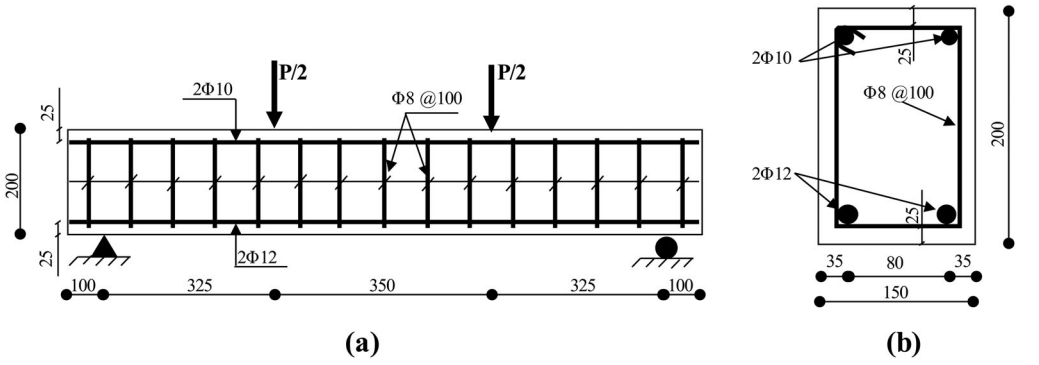

Figure 1. RC beam: (a) longitudinal view; (b) cross section. *Note:* all dimensions are in millimeters.

ultimate load capacities up to 153%, 108%, and 147% respectively, compared with that of the control beam.

In this study, a CFRP NSM, CFRP rope, hybrid system (CFRP NSM- and CFRP sheet), and hybrid system (CFRP rope and FRP sheet) system were introduced for the flexural strengthening of RC beams. This study aims to investigate experimentally and numerically the effectiveness of different techniques of CFRP for strengthening RC beams tested under flexural and evaluate the effect of different techniques including CFRP NSM, CFRP rope and hybrid system (CFRP NSM/rope and CFRP sheet) on the structural performance of RC beams. Moreover, this study aims to evaluate the effect of the amount of CFRP-NSM and CFRP rope on the flexural behavior of RC beams and asses the efficiency in terms of load-displacement behavior, mode of failure and capacity/cost ratio. This paper provides experimental evidence and detailed performance of various FRP strengthening techniques toward a design guidelines. Also, the cost analysis is provided for each technique in order to help engineers to judge the cost effectiveness of each system.

To achieve this objective, eight RC beams have been constructed and tested. Six of which strengthened using previous three techniques and two of which are control (unstrengthen) specimens. Four-point bending tests with RC beams were carried out under monotonic loading. The strengthened specimens were mainly categorised CFRP NSM strengthened specimens, CFRP rope strengthened specimens and hybrid system (CFRP NSM/rope and CFRP sheet) strengthened specimens. The outcomes of this work may be beneficial for researchers in the RC strengthening using FRP domain. Complementary to experimental work a non-linear finite element package by ABAQUS is used to investigate the flexural behaviour of the strengthened RC beam by CFRP NSM, CFRP rope and hybrid system (CFRP NSM/rope and CFRP sheet).

2. Experimental program

This section is fully described all details of the experimental work of strengthened RC beams. This work was conducted at the structures laboratory at Jordan University of Science and Technology (JUST). Eight RC beams were constructed and tested to investigate the effectiveness of using CFRP NSM, CFRP rope and hybrid system (CFRP NSM/rope and CFRP sheet) on the flexural behaviour of strengthened RC beams. Specifically, this section includes; material properties, preparation of RC beam specimens, casting and curing of the RC beam specimens, test setup and installation of CFRP-NSM, CFRP rope and FRP sheet to strengthen RC beams.

2.1. Specimens details

A total of eight simply supported RC beams were designed following ACI 318-2014 provisions (however, the spacing between shear links was selected 100 mm along the whole span of beams to make sure the beams' failure is in flexure) to appraise the effectiveness of the CFRP NSM, CFRP rope and hybrid system (CFRP NSM/rope and CFRP sheet) on the flexural behaviour of strengthened RC beams. All RC beam specimens were made of normal concrete with rectangular cross-section of (150 mm x 200 mm) (width x thickness) and length of 1200 mm (Figure 1). All RC beam specimens were longitudinally reinforced with

Table 1. Test Matrix.

Beam Designation	CFRP- strip	CFRP-Rope	CFRP-Sheet	Number of CFRP strip	Number of CFRP-Rope
Control	No	No	No	–	–
SB-NL1-SH0	Yes	No	No	1	0
SB-RL1-SH0	No	Yes	No	0	1
SB-NL1-SH1	Yes	No	Yes	1	0
SB-RL1-SH1	No	Yes	Yes	0	1
SB-NL2-SH1	Yes	No	Yes	2	0
SB-RL2-SH1	No	Yes	Yes	0	2

two deform bars of ϕ12 mm at bottom and two deform bars of ϕ10 mm at top. The transverse reinforcement was in terms of stirrups of ϕ8 mm at a spacing of 100 mm c/c to avoid shear failure. The rectangular stirrups had been supplied with a 50 mm overlap at their ends (Figure 1).

2.2. Strengthening configurations and test matrix

Two out of eight RC beams were used as control beams, however, the average of these beams were added in Tables and Figures "Experimentally two identical control RC beams were constructed and tested in this study to make sure that the test setup and LVDT's instrumentations were working properly which may lead to correct conclusions". The control RC beams were designed to have insufficient longitudinal steel reinforcement to make sure that the failure will be flexural failure in control beam. In this study there were two control beams reinforced with two main reinforcement T12. These beams were used to make a comparison with the strengthened beams to investigate the effect of using CFRP in turns of rope or strip or hybrid on flexural behaviour of RC beam. On another hand, the remaining six out of eight tested RC beam specimens were strengthened using CFRP NSM, CFRP rope and hybrid system (CFRP NSM/rope and CFRP sheet) to investigate their flexural behaviour. The designation of some RC beam specimens is in the format SB-RLx-SHx and some of them is in format SB-NLx-SHx. The abbreviations of letters in previous format as follows: The "SB" denotes for the strengthened RC beam; the second character "R or N" refers to the rope or NSM strip, respectively; the third character "SH" symbolises the CFRP sheet. Table 1 shows test matrix and specimens designation. Several configurations of CFRP-NSM, CFRP rope and CFRP sheet were used. One RC specimen beam was strengthened using one CFRP-NSM strip at bottom face of specimen as shown in Figure 2.a. One CFRP-rope was used to strengthen second beam (Figure 2.b). Two of RC beam specimens were strengthened by hybrid system which consists of (one CFRP-NSM and one layer of CFRP sheet) and (one CFRP rope and one layer of CFRP sheet) as shown in (Figure 2.c and Figure 2.d), respectively. The last two RC beam specimens were strengthened by hybrid system which consists of (two CFRP-NSM and one layer of CFRP sheet) and (two CFRP rope and one layer of CFRP sheet) as shown in (Figure 2.e and Figure 2.f), respectively. All attached CFRP-NSM, CFRP-rope and CFRP-NSM sheets have the same length of the beam and placed to tension soffit with span of 1200 mm. CFRP-sheet has width equal to width of RC beam specimen.

2.3. Material properties

All tested RC beams specimens were constructed with the identical concrete mix. A concrete mixture was designed according to the ACI-211 mix design procedure (American Concrete Institute, 1996) to attain a 28-day compressive cylinder strength of 32.8 MPa. Three concrete cylinders with 300 mm height and 150 mm diameter were tested to measure the compressive strength of concrete. The cylinders were tested under concentric load until failure to measure the concrete compressive.

The concrete compressive strength (f'c) was calculated by dividing the failure load by the cross-sectional area.

Three types of deformed bars with a diameter of 8 mm, 10 mm and 12 mm were used in reinforcing RC beam specimens. A two bars with 12 mm used at the bottom of RC beam and 10 mm used at the top of RC beam for the longitudinal steel reinforcement. Whereas, deformed steel bars with diameter of 8 mm was used for stirrups as shown in Figure 1. Tensile test was conducted on all diameters of steel bars at ambient temperature to measure their mechanical properties (Table 2).

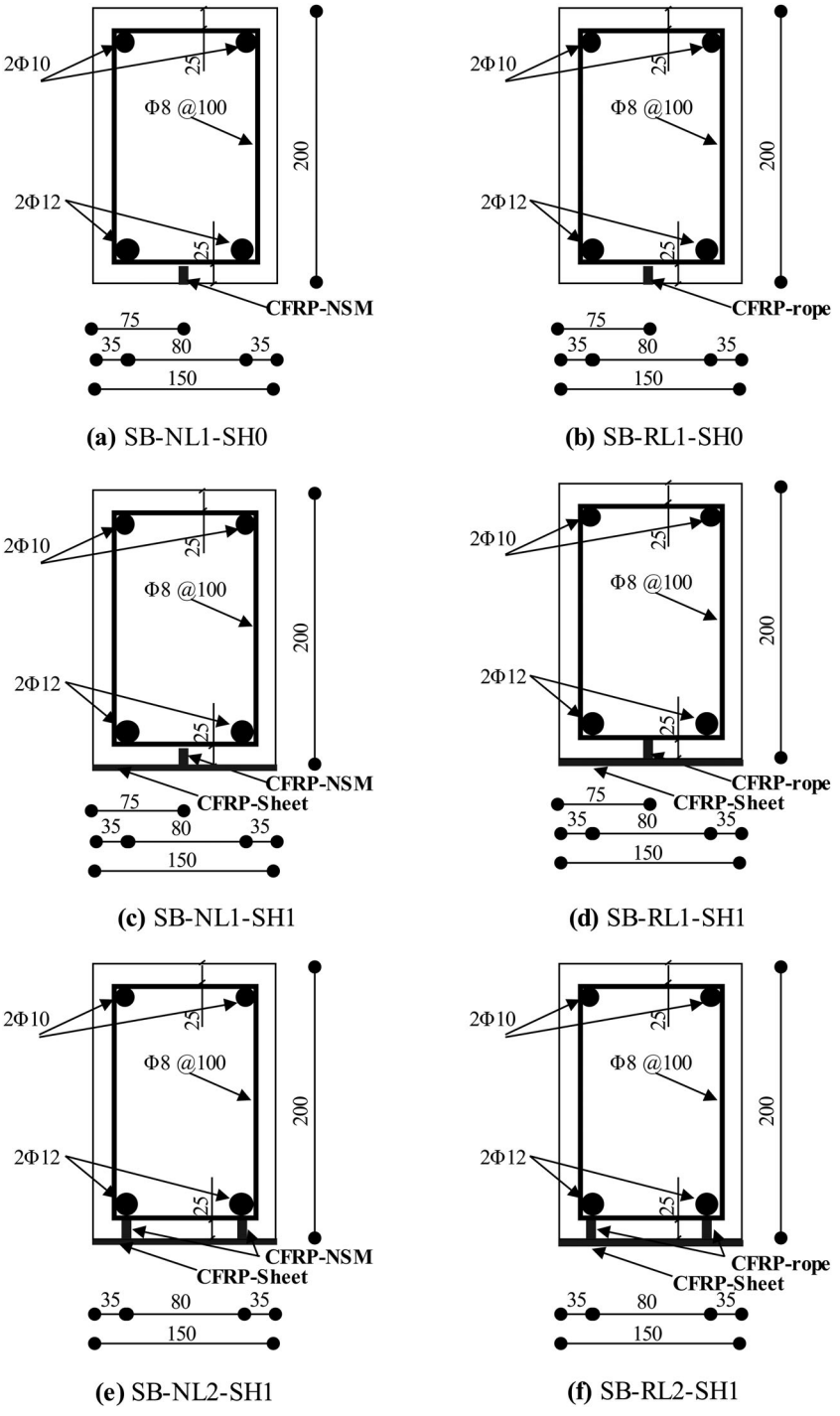

Figure 2. CFRP strip, CFRP strip and CFRP sheet strengthening configuration (Dimensions in mm).

Three products of CFRP were used in this study to strengthen six RC beam specimens in flexural (Figure 3). These CFRP products were including CFRP-strips, (CFRP) Wrap (NSM-CFRP rope) and sheet. Table 3 shows physical and mechanical properties of NSM CFRP Strips, Ropes and CFRP Sheet, respectively. In order to achieve an enough bond between CFRP strip and concrete surface in cut groove, an

Table 2. Mechanical properties of the reinforcing steel bars.

Nominal Bar Diameter	Actual Bar diameter	Yield Stress f_y (MPa)	Ultimate Stress, f_u (MPa)	Elongation at Failure (%)
10 mm	10.3	450.9	580.3	18
8 mm	8.1	542	683	16.2
12mm	12.3	420	560	18

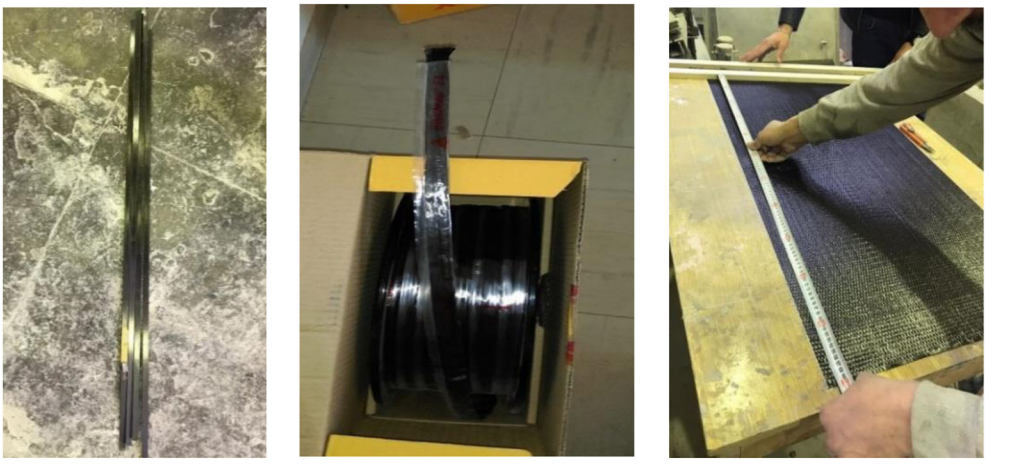

Figure 3. CFRP products used in this study.

Table 3. Physical and mechanical properties of NSM CFRP Strips.

	Strip NSM	CFRP Rope	CFRP sheet
Tensile E-modulus	165000 MPa	230'000 N/mm2	225'000 N/mm2
Elongation at break	1.7 %	1.6 %	1.7 %
Mean tensile strength	3100 MPa	4'000 N/mm2	3500 N/mm2

adhesive material with two components A and B of 6 kg with mix proportion 1:3 (1.5:4.5 kg) B to A, was used as recommended by the manufacturer. Material 52 LP was used as adhesive to fill the grooves in order to place CFRP rope with concrete. Material 52 LP adhesive having two parts, resin (part A) and hardener (part B). Material 52 LP was prepared by mixing part A and part B by weight with ratio 2 to 1. Meanwhile, Material 330 LP used to glue CFRP ropes and sheets and prepared by mixing two components, resin (part A) and hardener (part B) with ratio 4 to 1 parts by weight. Meanwhile, material 330 LP used to glue CFRP ropes and sheets. It was prepared by mixing two components A and B with ratio 4 to 1 parts by weight.

2.4. Concrete mixing, casting, and curing

Eight wooden molds were fabricated to cast the tested RC beam specimens. The steel reinforcement cage with 25 mm cover in all sides was previously prepared and then placed in the wooden mold as shown in Figure 4.a. For mixing the ingredients of concrete, a tilting drum mixer of 0.15 m^3 was used (Figure 4.b). The concrete mixture was poured in the wooden mold (Figure 4.c). The concrete was compacted using an electrical vibrator and the side was finished by a trowel to get a smooth surface.

2.5. Grooving RC beam specimens to install the CFRP strip and CFRP ropes

In order to install CFRP strip and rope, grooves in the concrete cover of RC beam specimens were made. The grooving with a depth of 20 mm and width of 9 mm was done by professional labours using grinder (electrical drill) into the concrete cover (Figure 5). The grooves were cleaned and washed from dust by a

a) Reinforcement cage in wooden mold **b)** Concrete mixing machine. **c)** Casting of RC beam specimens

Figure 4. Placing cage reinforcement, Concrete mixing and pouring of concrete.

a) One groove **b)** Two grooves **c)** Grinder **d)** Surface Cleaned With Vacuum Cleaner **e)** Beam Washed Using Thinner

Figure 5. Specimens Grooving.

vacuum cleaner "hoover". The RC beam specimens were then washed and cleaned using thinner to reduce the moisture and to create a stronger bond with CFRP ropes (Figure 5).

2.6. Installation of CFRP strip and rope

The following steps show how the CFRP strip and rope is embedded however, to be informed that that conducting CFRP in the Lab is different than site and this point is considered as a limitation of this research:

1. Cut out the CFRP strip and rope to length equal to the RC beam specimen length.
2. Material 52 LP and Material 330 LP resin to glued the CFRP strip and rope was prepared by mixing parts A and B with proportions of 2:1 and 4:1, respectively.
3. Material 52 LP resin was applied to CFRP rope with a sufficient amount to be saturated before entering the saturated rope into grooves.
4. The cut grooves made in concrete cover of RC beam specimen were filled with Material 330 LP resin using a plastic blade.
5. CFRP strip and rope were carefully placed into grooves.
6. Finally, the CFRP sheet was glued on the bottom surface of the RC beam specimens.

All steps from step one to step six are shown in Figure 6.

2.7. Test setup

All simply supported RC beam specimens were tested under four-point loadings up to failure using a load control criteria with a rate of 3.77 kN/sec. The load was applied using the Universal Testing Machine

Figure 6. CFRP strip and rope Installations.

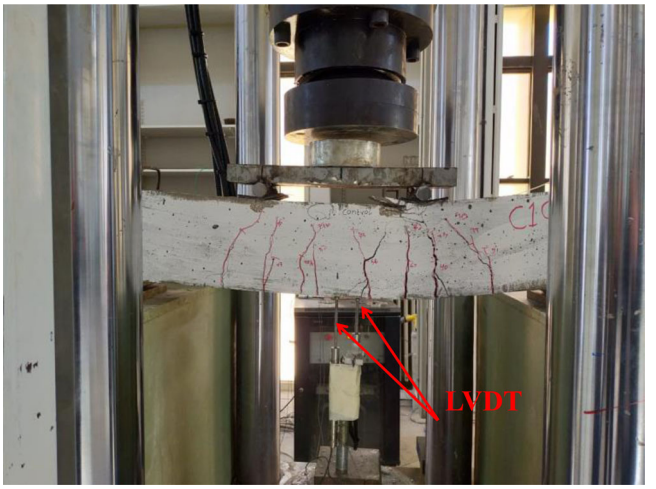

Figure 7. Two LVDT Installed on the beam.

(2000 kN capacity in compression) available at the structures laboratory at JUST. The fixed distance between the loads is 325 mm. Distance between support and load during test is fixed to 375 mm (Figure 1). All tested RC beam specimens were instrumented by two Linear Variable Differential Transformer (LVDT) at the mid of beam span from bottom surface in order to measure a deflection at mid of beam span during the testing (Figure 7). The load and displacement values were recorded by data acquisition system.

The test setup consisted of hydraulic cylinder which is attached by steel frame. This hydraulic cylinder applied the load through a 50 mm rigid steel plate in order to transfer the load into two rigid steel rods in which they transfer the load to the loading points (Figure 8). Load was measured by load cell that is placed under the hydraulic actuator. The rotation of the head of the actuator was allowed because the actuator is pinned. The beam was supported by roller and pin at a distance of 100 mm from ends of RC beam to prevent the translation in vertical direction and horizontal movement.

3. Results and discussion

The summary of the obtained experimental flexural test results in terms of (i) axial load, (ii) mid-span deflection corresponding to axial load capacity (δy), (iii) failure load (Pf), mid-span deflection

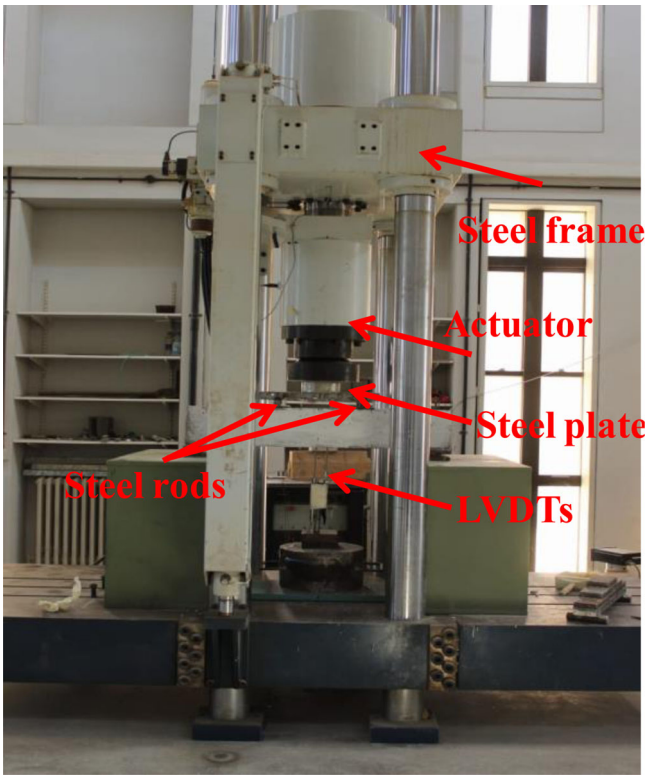

Figure 8. Test set up.

Table 4. Experimental results of RC beam specimens.

Specimen	P_u (kN)	%Pu (kN) Increase over Control	δu (mm)	% δu (mm) increase over Control	Pf (kN)	%Pf (kN) increase over Control	δf (mm)	% δf (mm) decrease over Control	Type of Failure
Control	71.35	–	2.53	–	90.5	–	26	–	Flexural
SB-NL1-SH0	129.7	80.8	7.74	206	123	36	19	27	Flexural
SB-RL1-SH0	127	76.3	8.75	246	99.5	10	26.6	−2.3	Flexural
SB-NL1-SH1	159.8	124	8	216	115	27	25	3.85	Flexural
SB-RL1-SH1	170	139	8.77	247	126	39	26	0	Flexural
SB-NL2-SH1	169.5	137.6	6.25	147	125	38	17	34.6	Flexural-Shear
SB-RL2-SH1	173.7	143.5	6.44	154	134	48	17.2	33.9	Flexural-Shear

corresponding to failure load (δf) and (iv) a summary of the type of final observed failure for each RC beam specimen (mode of failure) are detailed in Table 4. The control beam specimen was used as references for evaluating the performance of other strengthening RC beam specimens. Table 4 shows the percent increase of axial load (%Pu), percent increase of failure load (%Pf), percent increase of mid-span deflection corresponding to the axial load (%δu) and percent decrease of mid-span deflection corresponding to the failure load (%δf) compared to control RC beam specimen.

3.1. Flexural load carrying capacity

The flexural capacities of the control beam (un-strengthened) and strengthened RC beam specimens in terms of first cracking and ultimate load are shown in Figure 9. Figure 9 shows that the strengthened RC beam specimens by the hybrid system of CFRP exhibited a significant influence on the stiffness of the un-cracked section. The CFRP hybrid system improved noticeably the first cracking and axial load carrying capacities by up to 2.25 times and 2.38 times, respectively, as the control RC beam specimen. Hosen et al. (2018) showed that using SNSM-CFRP strips significantly improved the first cracking and ultimate load

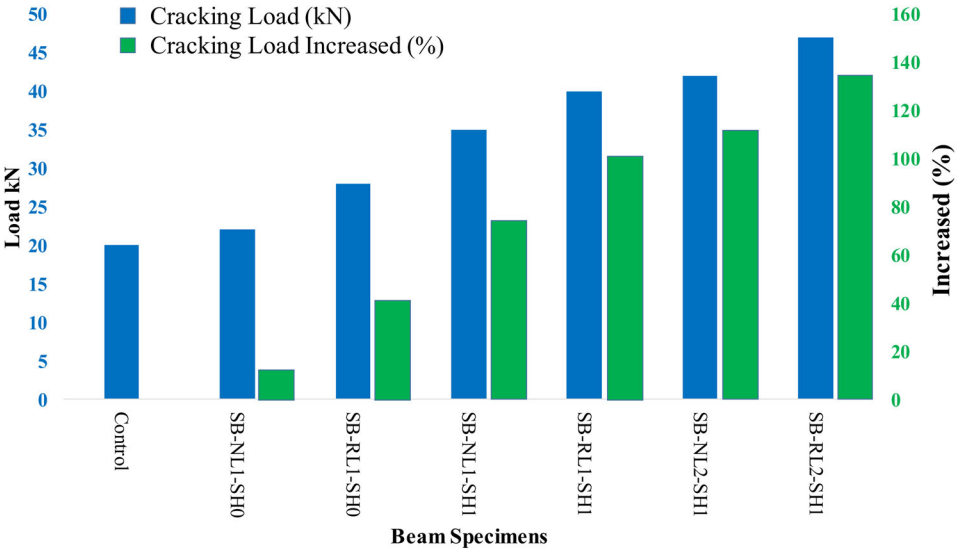

a) First Cracking Load

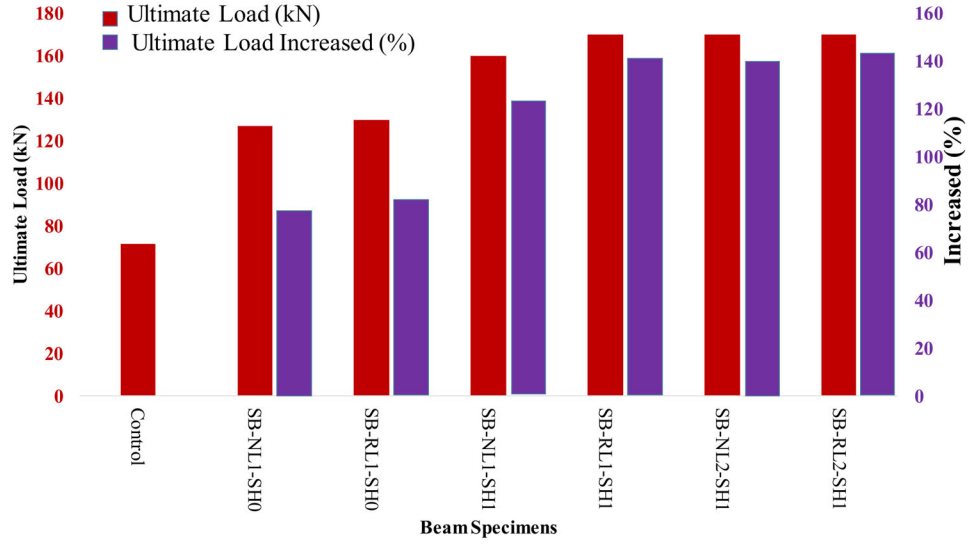

b) Ultimate Loads

Figure 9. First cracking and ultimate load carrying capacity of the specimens.

carrying capacities by up to 2.53 times and 2.47 times, respectively, compared with the control specimens. Hence, this conclusion almost similar to the Hosen et al. (2018). It can be noted that as the hybrid system of CFRP showed significantly increase in first cracking and axial load carrying. The increase in first cracking and axial load carrying in specimens SB-NL1-SH0, SB-RL1-SH0, SB-NL1-SH1, SB-RL1-SH1, SB-NL2-SH1 and SB-RL1-SH1 were (10%,78%),(40%, 82%),(75%, 124%), (100%, 138%), (110%, 138%) , (135%, 144%), respectively, compared with the control beam.

The strengthening of the RC beam specimens using two CFRP strip and ropes at the tension side exhibited an increase in the first cracking up to 100% as control beam specimen. This conclusion similar

Table 5. Cost analysis of CFRP.

Specimen	P_u (kN)	Increase over Control (kN)	Total cost CFRP length (cost of CFRP)	Cost/ Increase over control
Control	71.35	–	–	–
SB-NL1-SH0	129.7	58.35	1.2*28 = 33.6	0.575835
SB-RL1-SH0	127	55.65	1.2*17 = 20.4	0.366577
SB-NL1-SH1	159.8	88.45	1.2*28 + 0.18*28 = 38.64	0.436857
SB-RL1-SH1	170	98.65	1.2*17 + 0.18*28 = 25.44	0.257881
SB-NL2-SH1	169.5	98.15	1.2*2*28 + 0.18*28 = 72.24	0.736016
SB-RL2-SH1	173.7	102.35	1.2*2*17 + 0.18*28 = 45.48	0.444358

to Hosen et al. (2018) conclusion. In contrast, the RC beams strengthened with CFRP rope exhibited increase in and axial capacity loads up to 130% compared to the control specimen which more than increase concluded by Hosen et al. (2018).

3.2. Load deflection responses

In this study several techniques of CFRP configurations were used to strengthen the RC beam specimens as shown in Figure 2. All results obtained from experimental works for all tested RC beam specimens in terms of maximum axial load, deflection corresponding to the maximum load, failure load, deflection corresponding to the failure load, total cost of FRP length, Capacity/Cost and failure mode are summarised in Table 5. As shown in Figure 10, specimen strengthened using one layer of CFRP NSM strip (SB-NL1-SH0) exhibited maximum load similar to specimen strengthened using one layer of CFRP rope (SB-RL1-SH0) with toughness more than SB-RL1-SH0 specimen. Specimen strengthening using hybrid system of one layer of CFRP rope and CFRP sheet (SB-RL1-SH1) exhibited maximum load of 18.8% more than specimen strengthening using hybrid system of one layer of CFRP NSM strip and CFRP sheet (SB-NL1-SH1)with toughness more than SB-NL1-SH1 specimen as shown in Figure 11. Finally, Specimen strengthening using hybrid system of two layer of CFRP rope and CFRP sheet (SB-RL2-SH1) showed increase in strength about 2.5% more than specimen strengthening using hybrid system of two layer of CFRP NSM strip and CFRP sheet (SB-NL2-SH1) with toughness more than SB-NL2-SH1 specimen as shown in Figure 12. Furthermore, the SB-RL2-SH1and SB-NL2-SH1specimens have changed the type of failure of the strengthened specimens from pure flexural to a flexural shear failure. This can be attributed that the SB-RL2-SH1and SB-NL2-SH1 specimens have strengthened in flexural with hybrid system which in turn increase the flexural capacity and change the specimens to shear govern.

The experimental load–mid-span deflection relations for all tested specimens are shown in Figure 10, 11, 12, 13 and 14. It can be seen in the curves in these Figures an approximate linear response defined by pre-cracking, cracking (from first cracking to steel yielding) and post-cracking stages (from steel yielding to failure of the beam) (except SB-NL2-SH1). The linear elastic behaviour are showed in the strengthened RC beam specimens similar to the control beam. In the cracking stage, the stiffness and yielding load in the specimens strengthened by the CFRP NSM, rope and CFRP hybrid were increases. Finally, in the post cracking stage, all the strengthened specimens by CFRP exhibited axial load and deflection at midspan more than first two stages. The cracks was control by CFRP ropes and strip in this stage (except the SB-NL2-SH1). As such, in the cracking stage, the curve exhibited by SB-NL2-SH1 specimen was different.

3.2.1. Effect of CFRP type

It can be seen from Figure 10 that the strengthened RC beam specimens exhibited larger load capacity and strain corresponding to maximum load than those in control RC beam specimens. Figure 10 shows that the increase in maximum load in specimens SB-NL1-SH0 and SB-RL1-SH0 are 80.8% and 76.3%, respectively more than the control RC specimens. On another hand, Xing et al (2018) shows that using one bar of Basalt-fibre-reinforced polymers (BFRPs) in strengthening RC beam at bottom sides increased the maximum load about 111% more than the control RC specimen. Also, It can be observed that such increase in maximum load is an agreement with the experimental study that conducted by Hawileh et al. (2014). However, SB-NL1-SH0 and SB-RL1-SH0 specimens provided increase in maximum strain corresponding maximum load of 206% and 246%, respectively more than the control specimens.

The average maximum load Pu of the control RC specimen that was not strengthening by FRP was 71 kN. The SB-NL1-SH0 and SB-RL1-SH0 specimens increased the maximum load from 71 kN to 129.7 kN

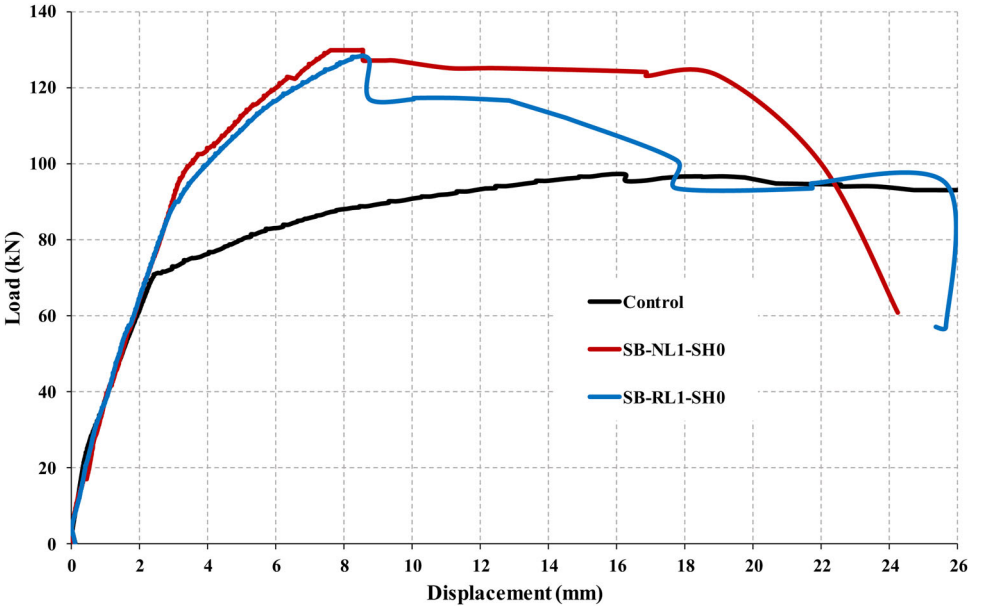

Figure 10. Load versus mid-span deflection for the control, SB-NL1-SH0 and SB-RL1-SH0 specimens.

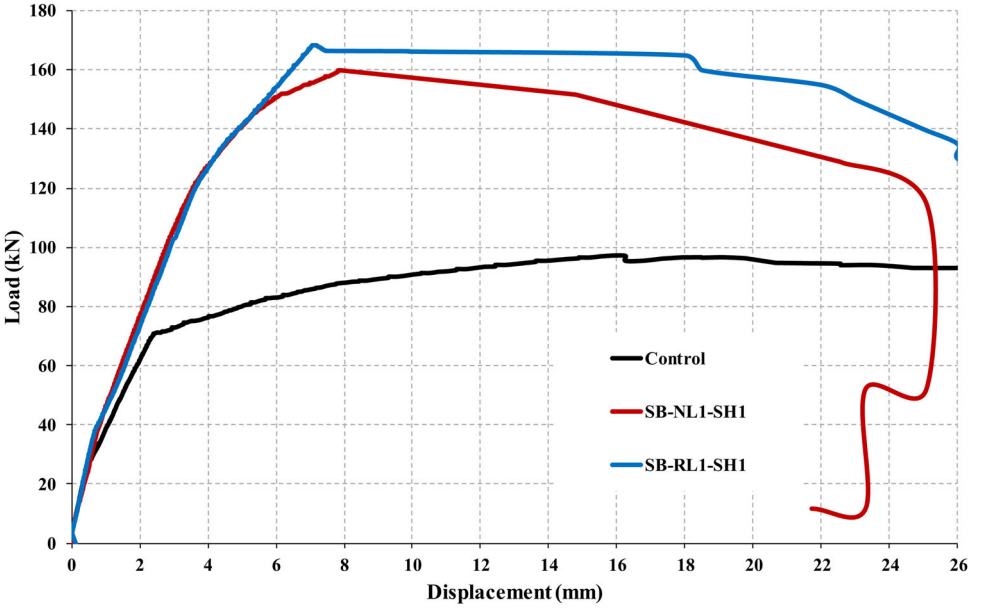

Figure 11. Load versus mid-span deflection for the control, SB-NL1-SH1 and SB-RL1-SH1 specimens.

and 127 kN, respectively. This means that the CFRP NSM and CFRP rope techniques contributed a load of 58.7 kN and 56 kN, respectively. This increase in load can be attributed to adding CFRP NSM and rope, respectively.

3.2.2. Effect of CFRP strengthening configuration

The increase in maximum load in SB-NL1-SH1 and SB-NL2-SH1 specimens was 124% and 137.6%, respectively more than maximum load in control specimens as shown in Figure 13 and Table 4. Meanwhile, it

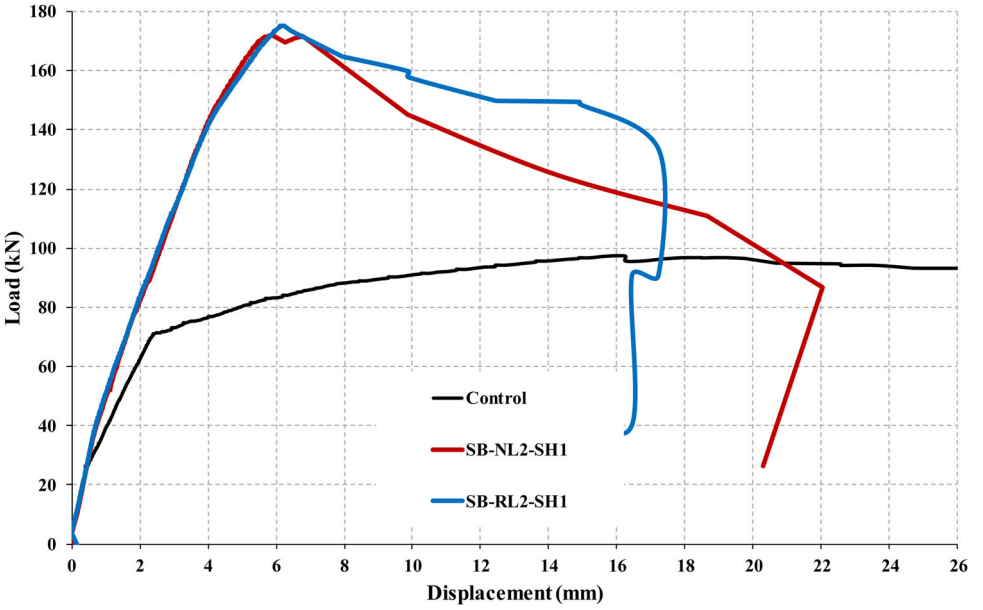

Figure 12. Load versus mid-span deflection for the control, SB-NL2-SH1 and SB-RL2-SH1 specimens.

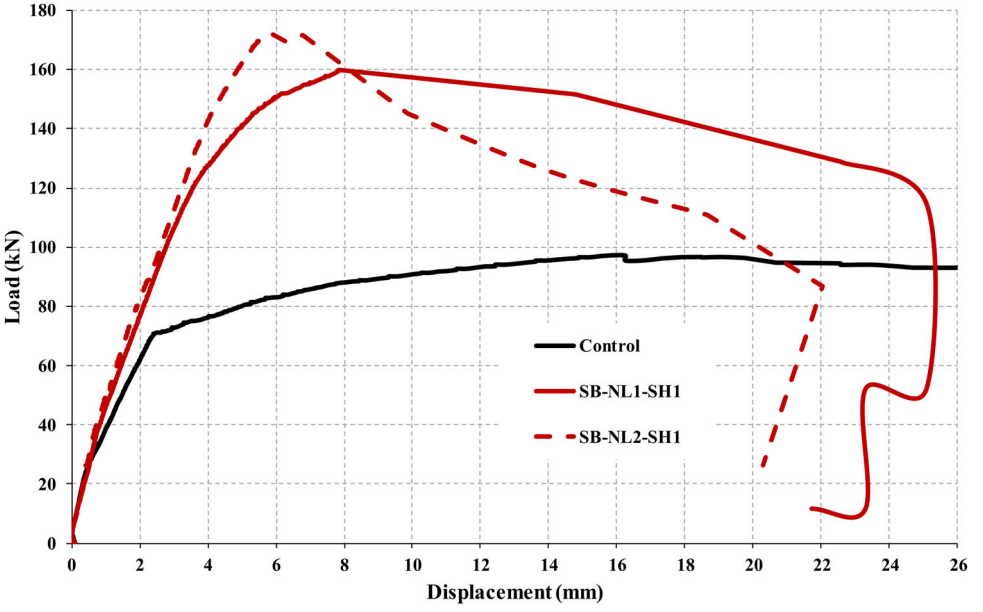

Figure 13. Load versus mid-span deflection for the control, SB-NL1-SH1 and SB-NL2-SH1 specimens.

can be seen in Figure 14 and Table 4that the SB-RL1-SH1 and SB-RL2-SH1specimens exhibited increase in maximum load about 139% and 143.5% of the control RC beam specimens. The SB-NL1-SH1, SB-NL2-SH1, SB-RL1-SH1 and SB-RL2-SH1 specimens increased the maximum load from 71 kN to 159.8 kN, 170 kN, 169.5 kN and 173.3 kN respectively. It can be observed that the SB-NL2-SH1 and SB-RL2-SH1 did not increase the maximum load significantly compared the load increase in SB-NL1-SH1 and SB-RL1-SH1as control specimens. It can be attributed that using two CFRP strip or CFRP rope require two grooves in concrete cover which in turn decrease the area of concrete. Consequently, decreasing the area of concrete increasing the stress concentration which lead to debonding in CFRP.

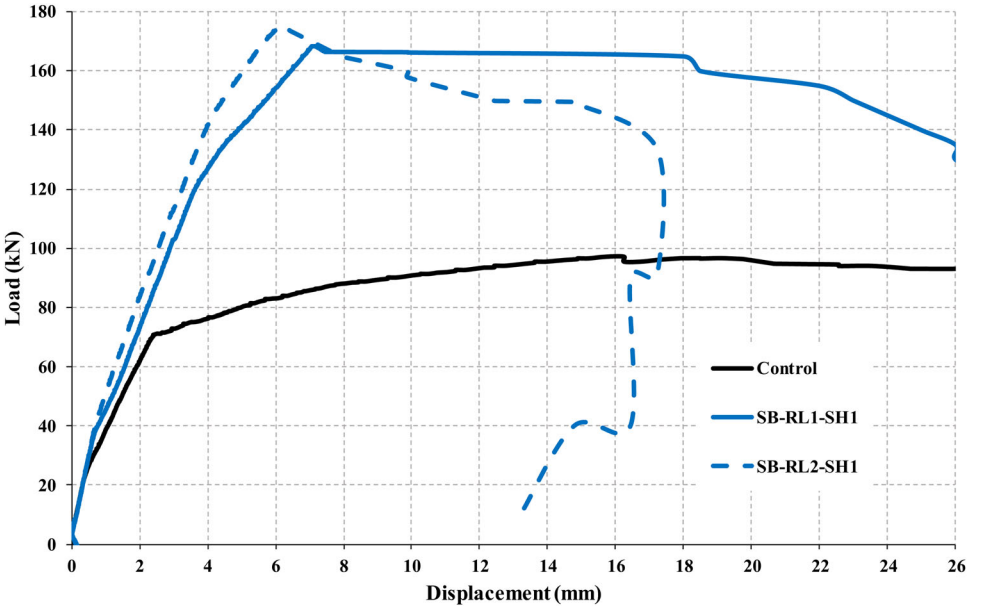

Figure 14. Load versus mid-span deflection for the control, SB-RL1-SH1 and SB-RL2-SH1 specimens.

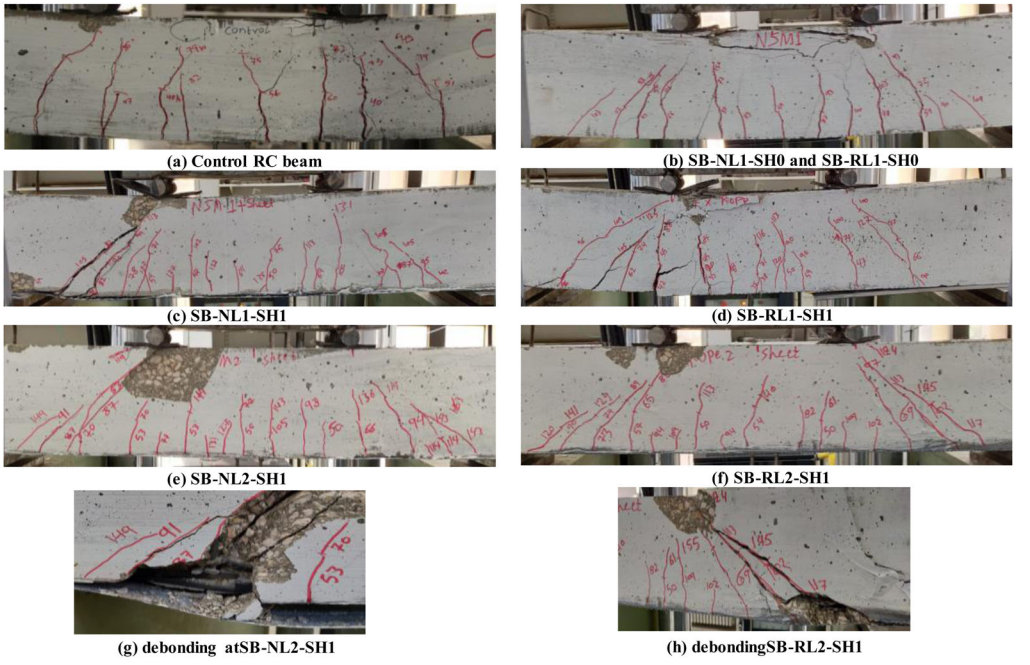

Figure 15. Crakes and Failure Mode of RC Beam specimens at failure.

3.3. Failure modes

Figure 15 shows the failure modes of the tested RC beam specimens. Different failure modes were observed in tested RC beam specimens such as flexure cracks, flexural shear cracks, debonding and concrete crushing. The failure mode of control RC specimen was in a flexural mode. This Flexural failure was happened toward the midspan of the RC beam by the spreading of a vertical crack. As the external applied load increased, the additional cracks developed, the cracks growth both in width and length, the

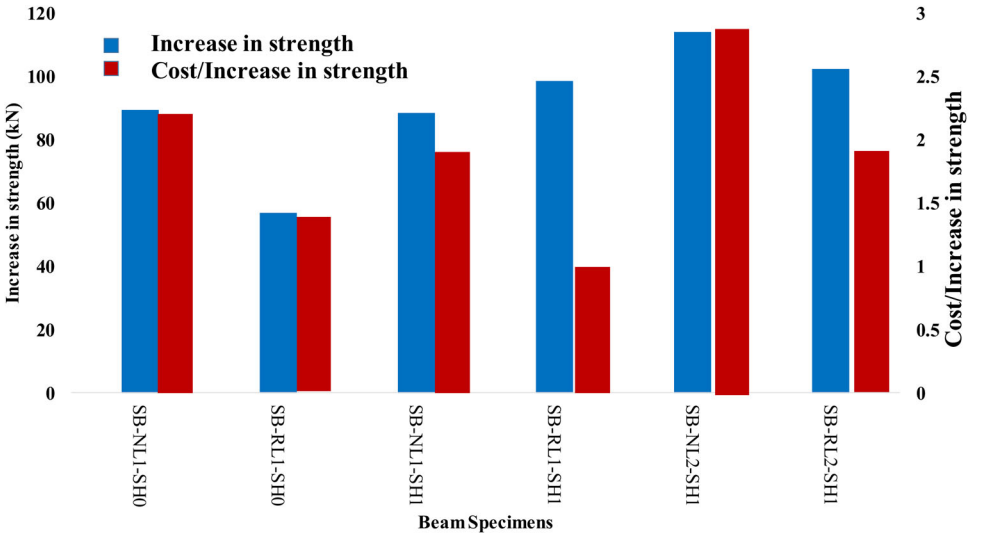

Figure 16. Cost analysis of various strengthening techniques.

deflection increases and further extend to the compression side as it moves to the upper part of the beam toward the loading point. This failure started by forming hair cracks at midspan then spread as the load increasing toward the natural axis of the specimen followed by yielding of flexural bottom steel reinforcement and eventually failed by concrete crushing at the extreme fibre of the specimen.

First crack appear on control RC beam specimen at 40 kN and failed at load of 75 kN. The maximum deflection corresponding peak load was 2.37 mm. RC beam specimens (SB-NL1-SH0, SB-RL1-SH0, SB-NL1-SH1 and SB-RL1-SH1) showed same flexural mode. The failure mode of these specimens are depicted in Figure 9 (b to d). It should be noted that there was no debonding in the CFRP materials in these specimens. The control specimen was shown similar failure mode in the study conducted by Xing et al (2018).

Finally, failure mode for the RC beam specimens (SB-NL2-SH1 and SB-RL2-SH1) was similar to (SB-NL1-SH0, SB-RL1-SH0, SB-NL1-SH1 and SB-RL1-SH1) (Figure 15 (e and f)). However, these specimens were failed by developing the flexural-shear cracks in the area at both sides close to the location of the point loads followed by delamination between CFRP sheet and concrete as shown in Figures 15 (g and h). The debonding was initiated when the diagonal shear crack intersected the flexural shear crack due to shear and normal interfacial stresses. Finally, these specimens as mentioned previously, failed by delamination due to edge cover separation from CFRP sheet. This is because the distance from the concrete edge to the center of the NSM CFRP, which was about 20 mm including the groove. This can be attributed to increasing the tensile strength of tensile zone which in turn decrease the strain at this zone which lead to convert the beam to compression controlled or transition failure.

3.4. Comparison between CFRP rope and strip strengthening technique considering effect of cost/increase in strength ratio

One of the main objectives of this study is to provide a best technique considering the cost-efficient. The efficiency is a function of the CFRP cost and the increase in strength over control specimen due to using of CFRP.

The economical strengthening configuration considering the costs of CFRP in terms cost/increase over control ratio are analyzed herein since the labour cost and tools needed to prepare concrete surface varies significantly among difference regions. Based on the local market, the cost of CFRP sheet/m^2 is 28 $and the CFRP strips cost per meter is 28$while the CFRP rope cost per meter is 17$. The cost of CFRP materials required for strengthening RC beam specimen with dimension of 150 mm x 200 mm x1200 mm were calculated and listed in Table 5 and Figure 16. In this study, Cost-efficiency was assessed in terms of CFRP length cost per increase in axial load capacity over control. It can be seen that in all configurations, the cost/increase over control ratio of specimens strengthened by CFRP rope was not significant as

the specimens strengthened by CFRP NSM strip. The specimens strengthened by CFRP rope was the most cost-efficient, with a cost/increase over control ratio of 0.6366 (less than 0.365 of the CFRP strip specimen), even though CFRP rope specimen exhibited maximum load less than the CFRP strip specimen. Hence, to obtain the same strengthening effect, the CFRP rope strengthened specimen cost nearly 65% of the cost of the CFRP strip strengthened specimen. Considering the axial load capacity of specimens, the specimen strengthened by hybrid system SB-RL1-SH1 (one layer of CFRP rope and CFRP sheet) showed a most economic technique strengthening. The specimens SB-NL1-SH10, SB-RL1-SH0, SB-NL1-SH1, SB-NL2-SH1 and SB-RL2-SH1 exhibited a cost/increase over control ratio about 2.23, 1.42, 1.69, 2.85 and 1.72 more than the specimen SB-RL1-SH1. It can be concluded that the CFRP rope has a good cost/increase over control strength, however, the cost of CFRP strip and CFRP rope in the local market is 28$and 17$, respectively, meaning the cost of CFRP rope was 40% lower than CFRP strip when the same strengthening effect was achieved. Please note that the CFRP rope production industry is relatively new and its price may be potentially decrease significantly, thereby using CFRP strip for strengthening specimens will be more cost-efficient. Finally, once the quality and the strength of CFRP are enhanced, the efficiency of CFRP in terms of strength and cost could be further improved.

4. Finite element analysis and results

4.1. Modelling

FEA Model in this study consisted mainly of seven parts. These parts represent the beam specimen, main bottom longitudinal reinforcement, main top longitudinal reinforcement, stirrups, CFRP (rope), CFRP (strip) and CFRP (sheet). As the experimental, the concrete beam was with square section of dimensions 150 mm x 200 mm and extrusion of 1100 mm. The bottom and top longitudinal reinforcement model as a wire of 1100 mm length and with diameter of 12 mm and 10 mm, respectively. The stirrups reinforcement was with diameter of 8 mm and model as a wire. The CFRP rope had a cross-section with dimensions of 10 mm x 20 mm with extrusion of 1100 mm. The CFRP strip had a cross-section with dimensions of 8 mm x 15 mm with extrusion of 1100 mm. Finally, the CFRP (sheet) had a cross-section with dimensions of 150 mm and 0.167 mm and extrusion of 1100 mm.

4.2. Constitutive model

In this FEA model, the damage plasticity model from ABAQUS was utilised to simulate the behaviour of concrete beam. In addition to the parameters of the concrete damage plasticity, the values of the modulus of Elasticity and Poisson's ratio are required for plastic damage model. The parameters of the concrete plastic damage were used for concrete beam are as following: the dilation angle of 36, the plastic potential eccentricity (0.1), the ratio of the strength in the biaxial state to the strength in the uniaxial state (1.16), the ratios of the distance between the hydrostatic axis and the compression meridian and the tension meridian, separately, in the deviatoric cross section (0.667), and the viscosity parameter that defines viscoplastic regularisation (0) (ACI 440F, 2008; Al Rjoub et al., 1988; Ashteyat et al., 2019; Kmiecik & Kamiński, 2011). The bond between the concrete and steel reinforcement is assumed to be perfect. This was done using the command of embedded regions available in the ABAQUS library.

The stress strain relationship proposed by Tsai equation (Tsai, 1988) was used to model the stress-strain behaviors of the concrete under uniaxial compression. Equation 4.1 describes the Tsai Equations.

$$f_c = \frac{n\frac{\varepsilon_c}{\varepsilon_c'}}{1+\left(n-\frac{r}{r-1}\right)\frac{\varepsilon_c}{\varepsilon_c'}+\frac{\left[\frac{\varepsilon_c}{\varepsilon_c'}\right]^r}{r-1}} f_c' \qquad \text{where } n=\frac{E_c\varepsilon_c'}{f_c'},\ E_c=4700\sqrt{f_c'} \text{ and } r=\frac{f_c'}{750}-1.9 \tag{4.1}$$

where

f_c', ε_c' and E_c are the compressive strength of the concrete, the corresponding strain to the concrete compressive strength and the initial modulus of elasticity which is calculated using ACI equation, respectively. However, the concrete tensile stress-strain behaviour is modelled based on Tsai's equation (Tsai, 1988).

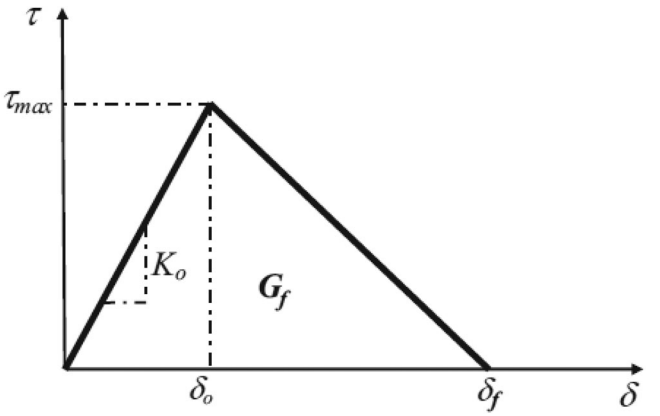

Figure 17. Bilinear traction-separation constitutive law.

Equation 4.2 describes the Tsai Equations.

$$\frac{f_t}{f_{to}} = \frac{n\frac{\varepsilon_t}{\varepsilon_{to}}}{1+\left(n-\frac{r}{r-1}\right)\frac{\varepsilon_t}{\varepsilon_{to}}+\frac{\left[\frac{\varepsilon_t}{\varepsilon_{to}}\right]^r}{r-1}} f_c' \qquad (4.2)$$

$$\text{where } n \text{ was taken as } 1.15 \text{ and } r = \frac{f_c'}{750} - 1.9$$

Reinforcement stress-strain behaviour was simulated using plastic model from the ABAQUS software. Stress-strain behaviour of steel reinforcement is defined with a Young modulus of elasticity of 200,000 MPa and Poisson's ratio 0.3. The bottom reinforcement, top reinforcement and stirrups had a yield strength of 468 MPa, 420 MPa and 248 MPa, respectively with zero corresponding plastic strain.

In this model three techniques of strengthening were used. The NSM CFRP strips, ropes and sheets are modelled as an isotropic linear elastic material with a Tensile Modulus of 165000 MPa, 230000 MPa and 225000 MPa, respectively.

4.3. Interaction modeling

Interaction (cohesive) Behaviour between NSM CFRP strips or ropes or sheets and concrete is modelled using traction-separation modeling procedure. The separation distance between interface elements traction function was defined using the traction separation law as illustrated in Figure 17. Interaction (cohesive) behaviour is applied between surfaces of CFRP material and concrete. The interaction between these surfaces is represented by interaction (cohesive) behaviour based on traction versus separation law. The failure of cohesive interface and reduction in cohesion is simulated by modelling the damage over two steps: damage initiation and damage evolution.

The adhesive is initially had a linear elastic behaviour. Thereafter, the damage initiation and evolution is occurred until total degradation of the elements. This was done by the quadratic stress-based damage initiation criterion available in ABAQUS. This criterion was defined by two parameters: the normal stress limit that equal to the tensile concrete strength that calculated according to ACI code (American Concrete Institute, ACI Committee 318, 2011) and the maximum shearing stress (MPa) components that calculated according to Eq. (4.1) (Zhang et al., 2013). Whereas, fracture energy (N.mm) parameter and a power coefficient equal to 1.45 were used to define the damage evolution which calculated by Eq. (4.2) (Benzeggagh & Kenane, 1996).

$$\tau_{\max} = 1.15\gamma^{0.138} f_c^{0.613} \qquad 4.1$$

$$G_f = 0.4\gamma^{0.422} f_c^{0.619} \qquad 4.2$$

where γ is the groove height-to-width ratio, and fc is the concrete compressive strength in MPa.

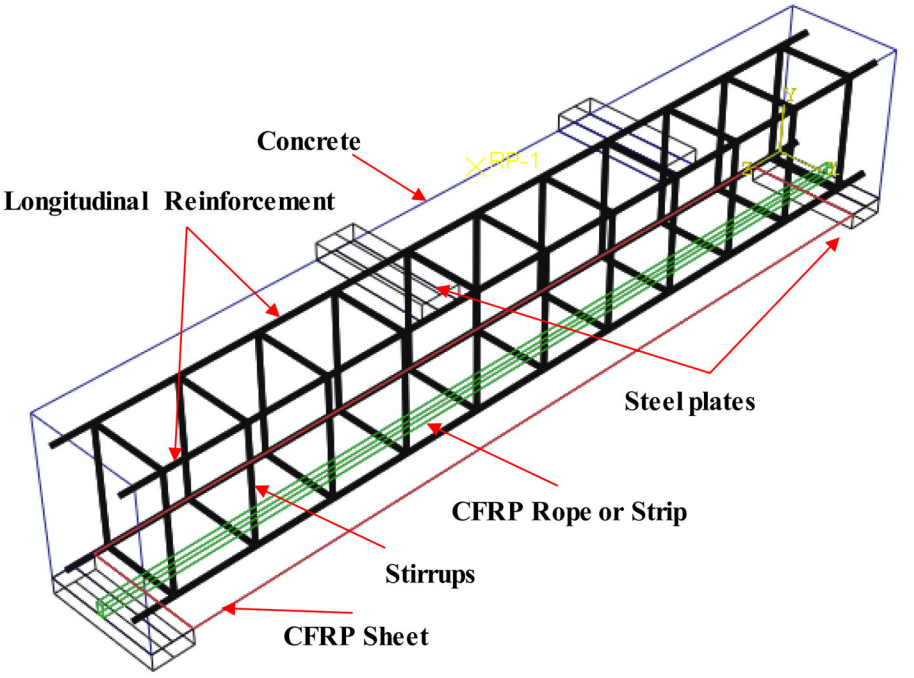

Figure 18. FEM model assemblage.

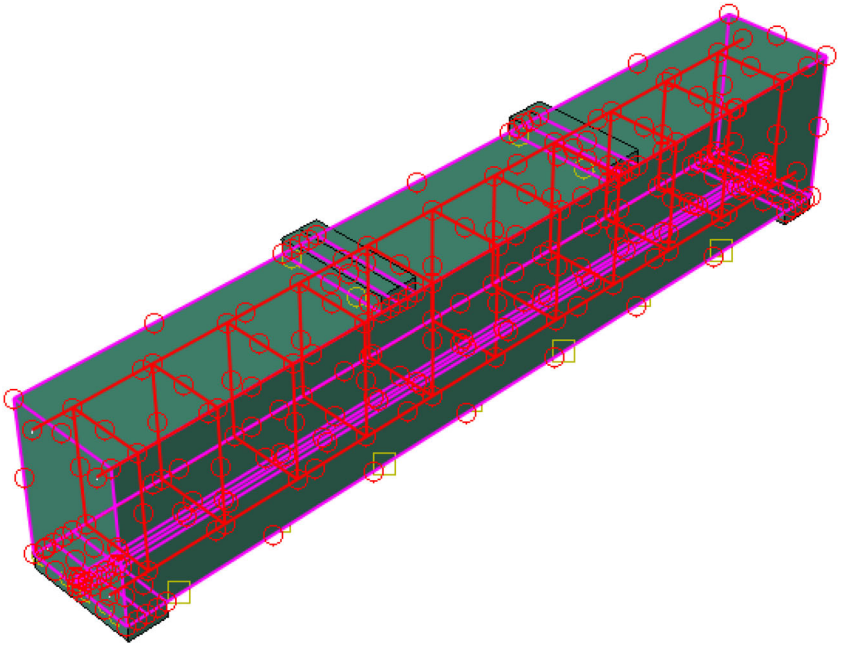

Figure 19. Interaction between materials.

In this model, Three-dimensional eight-node solid elements were used for the reinforcement bars, reinforced concrete, CFRP rope, strip and sheet and steel plates. As experimental work, all longitudinal, transverse (stirrups) reinforcement and CFRP materials were placed in their position (Figure 18).

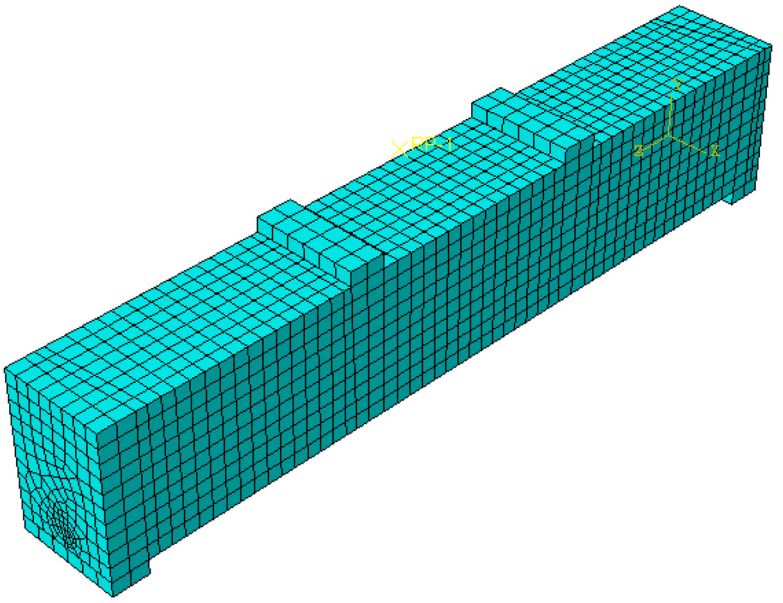

Figure 20. Element mesh size.

Two types of interface model were used in this model. First type is the perfect bond between steel reinforcement and concrete which has been implemented using embedded region command in ABAQUS (making beam component parts as one unit when applying the load. Second type is the interface cohesive model between concrete and CFRP materials as mentioned in previous section (Figure19).

Two boundary conditions (BC) were implemented in this model; Load, pinned and roller supports. The displacement load was applied at the top of the RC beam geometry using a reference point at the middle of RC beam. A multi-points connection (MPC) command available in the ABAQUS was used to apply a linear distributed load on two plates as experimental work. A Hex element shape mesh was used to mesh all parts with 20 mm size as shown in Figure 20.

4.4. Validation of the experimental and numerical results

Figure 21 shows the numerically calculated load-deflection curves for control, SB-NL1-SH0, SB-RL1-SH0, SB-NL1-SH1 and SB-RL1-SH1 specimens and the measured experimentally load-displacement relation curves of these RC tested beam. Four different techniques of CFRP materials for strengthening RC beams were used in this study. The curves in the Figure 21 show somehow a good agreement between the FEA model and experimental results for the control, SB-NL1-SH0, SB-RL1-SH0, SB-NL1-SH1 and SB-RL1-SH1 specimens. It can be seen that initially all beams were nearly exhibited the same linear behaviour until maximum load. However, FEA model showed an overestimates (FEM analysis predicts the beam to be slightly stiffer and stronger) in all RC beams compared with experimentally tested RC beams. The overestimates can be attributed to assumption of a perfect bond between reinforcement bars and concrete. Moreover, defining the behaviour of steel reinforcement, CFRP materials and compressive and tensile behaviour of concrete using analytical models exhibited a different results somehow than experimental results. In general, overall trend of the stress-strain curves show satisfactory agreement. It can be seen that adding CFRP sheet and CFRP ropes or strip significantly influences the flexural behaviour of the RC beam.

5. Conclusion

Experimental work and numerical FEA model were conducted to investigate the effect of different strengthening techniques of CFRP on flexural load-displacement behaviour of RC beams. Moreover,

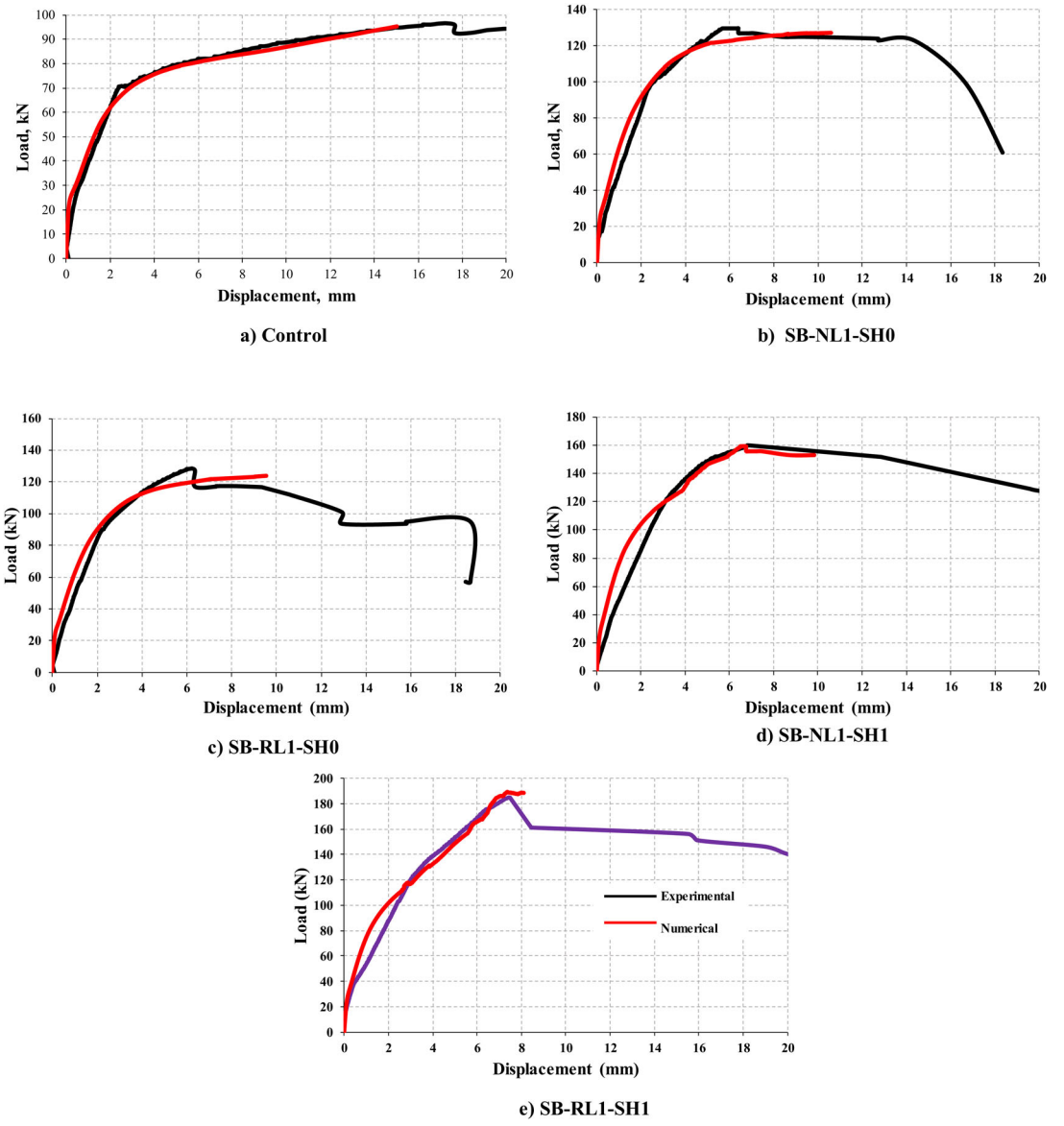

Figure 21. Load–deflection curves of RC beams, obtained by experiments and FEA model.

investigating experimentally and numerically the effectiveness of these techniques for strengthening RC beams tested under flexural in terms of strength and cost. Eight RC beams were constructed and tested under four point loadings until failure. In addition, an FEA model was developed using ABAQUS software to analyze beams strengthened with CFRP and validated with the experimental results including load-displacement behaviour. From this study, the following conclusions can be drawn:

- The control specimen and the RC beams specimens (SB-NL1-SH0, SB-RL1-SH0, SB-NL1-SH1 and SB-RL1-SH1) strengthened by one layer of CFRP strip or rope with and without CFRP sheet were failed in flexural mode as designed. However, the RC beams specimens (SB-NL2-SH1 and SB-RL2-SH1) strengthened by two layer of CFRP strip or rope with CFRP sheet were failed in flexural-shear mode.
- The strengthened RC beam specimens exhibited larger load capacity and strain corresponding to maximum load than those in control RC beam specimens. The average increase in capacity and strain corresponding to maximum load were 76.3% to 143.5% and 206% to 246%.

- Specimen strengthened using CFRP NSM strip (SB-NL1-SH0, SB-NL1-SH1 and SB-NL2-SH1) exhibited maximum load approximately similar to specimen strengthened using CFRP rope (SB-RL1-SH0, SB-RL1-SH1 and SB-RL2-SH1), respectively.
- The capacity/cost ratio of specimens strengthened by CFRP rope is 61% higher than the capacity/cost ratio of specimens strengthened by CFRP NSM strip.
- RC specimens strengthened by one layer of CFRP rope (SB-RL1-SH1) is the most economic strengthening configuration even though it exhibited maximum load less than the (SB-RL2-SH1 and SB-NL2-SH1) specimens.
- The CFRP rope techniques achieved the best strengthening effects and great cost-efficiency.
- The FEA model results showed somehow good agreement with the experimental results.

Acknowledgements

The author acknowledge the assistant by the technicians at the structural and materials laboratory via the Department of Civil Engineering at Jordan University of Science and Technology. Also my most grateful appreciation goes to Ahmed Ali AL-Qabarah, Baha Mohammad Obeidat, Saif Ahmed AL-Refai and Islam Haitham Khalil for their help and efforts to complete this work.

Disclosure statement

A disclosure statement reporting no conflict of interest has been inserted. Please correct if this is inaccurate.

References

ACI 440F. (2008). *Guide for the design and construction of externally bonded FRP systems for strengthening concrete structures* (Report ACI 440.2R-08). American Concrete Institute. (pp. 80).

Al Rjoub, Y. S., Ashteyat, A. M., Obaidat, Y. T., & Bani-Youniss, S. (1988). Shear strengthening of RC beams using near-surface mounted carbon fibre-reinforced polymers. *Australian Journal of Structural Engineering*, *144*(9), 54–62.

American Concrete Institute, ACI Committee 318. (2011). *Building Code Requirements for Structural Concrete Commentary (ACI 318R–011)*. American Concrete Institute.

American Concrete Institute. (1996). Standard practice for selecting proportions for normal, heavyweight, and mass concrete. ACI Manual of Concrete Practice, Part 1-1996. Detroit.

Ashteyat, A., Al Rjoub, Y., Obaidat, A. T., & Dagamseh, H. (2019). Strengthening and repair of one-way and two-way self-compacted concrete slabs using near-surface-mounted carbon-fiber-reinforced polymers. *Advances in Structural Engineering*, *22*(11), 2435–2448. https://journals.sagepub.com/doi/abs/10.1177/1369433219843649. https://doi.org/10.1177/1369433219843649

Ashteyat, A., Haddad, R., & Obaidat, Y. (2020, April). Repair of heat-damaged SCC cantilever beams using SNSM CFRP strips. *Structures*, *24*, 151–162. https://doi.org/10.1016/j.istruc.2020.01.005

Bakis, C. E., Bank, L. C., Brown, V. L., Cosenza, E., Davalos, J. F., Lesko, J. J., Machida, A., Rizkalla, S. H., & Triantafillou, T. C. (2002). Fiberreinforced polymer composites for construction-state-of-the-art review. *Journal of Composites for Construction*, *6*(2), 73–87. https://doi.org/10.1061/(ASCE)1090-0268(2002)6:2(73)

Benzeggagh, M. L., & Kenane, M. (1996). Measurements of mixed-mode delamination fracture toughness of unidirectional glass/epoxy composites with mixed-modebending apparatus. *Composites Science and Technology.*, *56*(4), 439–449. https://doi.org/10.1016/0266-3538(96)00005-X

Bilotta, A., Ceroni, F., Nigro, E., & Pecce, M. (2015). Efficiency of CFRP NSM strips and EBR plates for flexural strengthening of RC beams and loading pattern influence. *Composite Structures*, *124*, 163–175. https://doi.org/10.1016/j.compstruct.2014.12.046

De Lorenzis, L., & Teng, J. G. (2007). Near-surface mounted FRP reinforcement: an emerging technique for strengthening structures. *Composites Part B: Engineering* , *38*(2), 119–143. https://doi.org/10.1016/j.compositesb.2006.08.003

Dias, S. J. E., & Barros, J. A. O. (2017). NSM shear strengthening technique with CFRP laminates applied in high T cross section RC beams. *Composites Part B: Engineering*, *114*, 256–267. https://doi.org/10.1016/j.compositesb.2017.01.028

El-Hacha, R., & Rizkalla, S. H. (2004). Near-surface-mounted fiber-reinforced polymer reinforcements for flexural strengthening of concrete structures. *Structural Journal*, *101*(5), 717–726.

Grace, N., Abdel-Sayed, G., & Ragheb, W. (2002). Strengthening of concrete beams using innovative ductile fiber-reinforced polymer fabric. *ACI Structural Journal*, *99*(5), 692–700.

Hassan, T., & Rizkalla, S. (2003). Investigation of Bond in Concrete Structures Strengthened with Near Surface Mounted Carbon Fiber Reinforced Polymer Strips. *Journal of Composites for Construction*, *7*(3), 248–257. https://doi.org/10.1061/(ASCE)1090-0268(2003)7:3(248)

Hawileh, R., Rasheed, H., Abdalla, J. A., & Tamimi, A. (2014). Behavior of reinforced concrete beams strengthened with externally bonded hybrid fiber reinforced polymer systems. *Materials and Design*, *53*, 972–982. https://doi.org/10.1016/j.matdes.2013.07.087

Hosen, M. A., Jumaat, M. Z., Alengaram, U. J., & Sulong, N. R. (2018). CFRP strips for enhancing flexural performance of RC beams by SNSM strengthening technique. *Construction and Building Materials*, *165*, 28–44. https://doi.org/10.1016/j.conbuildmat.2017.12.052

Kim, H. S., & Shin, Y. S. (2011). Flexural behavior of reinforced concrete (RC) beams retrofitted with hybrid fiber reinforced polymers (FRPs) under sustaining loads. *Composite Structures*, *93*(2), 802–811. https://doi.org/10.1016/j.compstruct.2010.07.013

Kmiecik, P., & Kamiński, M. (2011). Modelling of reinforced concrete structures and composite structures with concrete strength degradation taken into consideration. *Archives of Civil and Mechanical Engineering*, *11*(3), 623–636. https://doi.org/10.1016/S1644-9665(12)60105-8

Li, L-j., Guo, Y-c., Huang, P-y., Liu, F., Deng, J., & Zhu, J. (2009). Interfacial stress analysis of RC beams strengthened with hybrid CFS and GFS. *Construction and Building Materials*, *23*(6), 2394–2401. https://doi.org/10.1016/j.conbuildmat.2008.10.006

Mirmiran, A., & Shahawy, M. (1997). Behavior of concrete columns confined by fiber composites. *Journal of Structural Engineering*, *123*(5), 583–590. https://www.researchgate.net/publication/239390760_Behavior_of_Concrete_Columns_Confined_by_Fiber_Composites. https://doi.org/10.1061/(ASCE)0733-9445(1997)123:5(583)

Obaidat, A. T., Ashteyat, A. M., Hanandeh, S., & Al-Btoush, A. Y. (2020). Behavior of heat damaged circular reinforced concrete columns repaired using Carbon Fiber Reinforced Polymer rope. *Journal of Building Engineering*, *31*, 101424. https://www.sciencedirect.com/science/article/pii/S2352710219327007?via%3Dihub. https://doi.org/10.1016/j.jobe.2020.101424

Obaidat, Y. T., Ashteyat, A. M., & Obaidat, A. T. (2020). Performance of RC Beam Strengthened with NSM-CFRP Strip Under Pure Torsion: Experimental and Numerical Study. *International Journal of Civil Engineering*, *18*(5), 585–593. https://doi.org/10.1007/s40999-019-00487-2

Olivova, K., & Bilcik, J. (2009). Strengthening of concrete columns with CFRP. *Slovak Journal 640 of Civil Engineering*, 1–9.

Sarafraz, M., & Danesh, F. (2008, October). Flexural enhancement of RC columns 642 with FRP. In The 14th World Conference on Earthquake Engineering, 1–7.

Szabó, Z. K., & L. Balázs, G. (2007). Near-surface mounted FRP reinforcement for strengthening of concrete structures. *Periodica Polytechnica Civil Engineering*, *51*(1), 33–38. https://doi.org/10.3311/pp.ci.2007-1.05

Tsai, W. T. (1988). Uniaxial compressional stress-strain relation of concrete. *Journal of Structural Engineering*, *114*(9), 2133–2129. https://doi.org/10.1061/(ASCE)0733-9445(1988)114:9(2133)

Wu, Z., Shao, Y., Iwashita, K., & Sakamoto, K. (2007). Strengthening of preloaded RC beams using hybrid carbon sheets. *Journal of Composites for Construction*, *11*(3), 299–307. https://doi.org/10.1061/(ASCE)1090-0268(2007)11:3(299)

Xing, G. H., Chang, Z. Q., & Bai, Z. Q. (2018). Flexural behaviour of RC beams strengthened with near-surface-mounted BFRP bars. *Magazine of Concrete Research*, *70*(11), 570–582. https://doi.org/10.1680/jmacr.17.00227

Xiong, G., Yang, J., & Ji, Z. (2004). Behavior of reinforced concrete beams strengthened with externally bonded hybrid carbon fiber-glass fiber sheets. *Journal of Composites for Construction*, *8*(3), 275–278. https://doi.org/10.1061/(ASCE)1090-0268(2004)8:3(275)

Xiong, G., Yang, J., & Ji, Z. (2004). Behavior of reinforced concrete beams strengthened with externally bonded hybrid carbon fiber–glass fiber sheets. *Journal of Composites for Construction*, *8*(3), 275–278. https://doi.org/10.1061/(ASCE)1090-0268(2004)8:3(275)

Zhang, S. S., Teng, J. G., & Yu, T. (2013). Bond-slip model for CFRP strips near-surface mounted to concrete. *Engineering Structures*, *56*, 945–953. https://doi.org/10.1016/j.engstruct.2013.05.032